

Robust Organogels from Nitrogen-Containing Derivatives of (*R*)-12-Hydroxystearic Acid as Gelators: Comparisons with Gels from Stearic Acid Derivatives[†]

V. Ajay Mallia,[‡] Mathew George,^{‡,||} Daniel L. Blair,[§] and Richard G. Weiss*,[‡]

[‡]Department of Chemistry and [§]Department of Physics, Georgetown University, Washington, D.C. 20057-1227 ^{||}Present address: Sepax Technologies, Inc., Newark, Delaware 19711.
Gels and Fibrillar Networks

Received December 23, 2008

Thirteen members of a new class of low molecular-mass organogelators (**LMOGs**), amides, and amines based on (*R*)-12-hydroxystearic acid (**HSA**; i.e., (*R*)-12-hydroxyoctadecanoic acid) and the properties of their gels have been investigated by a variety of structural and thermal techniques. The abilities of these **LMOGs**, molecules with primary and secondary amide and amine groups and the ammonium carbamate salt of 1-aminoctadecan-12-ol, to gelate a wide range of organic liquids have been ascertained. Their gelating efficiencies are compared with those of **HSA** and the corresponding nitrogen-containing molecules derived from stearic acid (i.e., **HSA** that lacks a 12-hydroxyl group). Several of the **HSA**-derived molecules are exceedingly efficient **LMOGs**, with much less than 1 wt % being necessary to gelate several organic liquids at room temperature. Generally, the self-assembled fibrillar networks of the gels consist of spherulitic objects whose dimensions depend on the protocol employed to cool the precursor sol phases. X-ray studies indicate that the **LMOG** molecules are packed in lamellae within the fibers that constitute the spherulites. In addition, some of the organogels exhibit unusual thixotropic properties: they recover a large part of their viscoelasticity within seconds of being destroyed by excessive strain shearing. This recovery is at least an order of magnitude faster than for any other organogel with a crystalline fibrillar network reported to date. Correlations of these **LMOG** structures (as well as with those that lack a hydroxyl group along the *n*-alkyl chain, a headgroup at its end, or both) with the properties of their gels, coupled with the unusual rheological properties of these systems, point to new directions for designing **LMOGs** and organogels.

Introduction

As a result of their potential applications and fundamental importance, gels made with low molecular-mass organic gelators (**LMOGs**) have experienced increasing interest in recent years.¹ The **LMOGs** self-assemble primarily by 1D growth modes² to form fibers, strands, or tapes via relatively weak physical molecular interactions such as van der Waals forces, intermolecular H bonding, electrostatic forces, $\pi-\pi$ stacking, or even London dispersion forces. How these weak physical interactions affect the formation, strength, and stability of a gel must be understood in order to design organogels with the desired properties.

The range of structures known to be **LMOGs** is extremely broad. It includes molecules as simple as *n*-alkanes^{3–5} (**a** in

Scheme 1) and as complex as substituted steroids or salts made by the addition of two components.^{1,6} Thus, London dispersion forces must play a dominant stabilizing role in networks made by the **LMOG**, *n*-hexatriacontane (**C36**),⁴ because it lacks the functional groups that are necessary for the other favorable intermolecular interactions. Carboxylic acids with long alkyl chains (e.g., **b** in Scheme 1), such as stearic acid (**SA**; i.e., octadecanoic acid), offer the possibility of additional intermolecular interactions (N.B., H bonding) within the **LMOG** assemblies. In that regard, when cooled below a characteristic temperature (T_g), solutions of relatively high concentrations of long-chained saturated fatty acids and their salts are known to form gelatinous materials with fibrous substructures.⁷

Structure **c** in Scheme 1 represents **LMOGs** with two different functional groups attached to an *n*-alkane. Interesting examples of such **LMOGs** with secondary amide groups are 11-(butylamido)undecanoic acid,⁸ the sodium salt of *N*-octadecyl maleamic acid (a hydrogelator),⁹ and *N*-3-hydroxypropylodecanamide¹⁰ as well as a naturally

*Corresponding author. E-mail: weissr@georgetown.edu.

[†]Part of the Gels and Fibrillar Networks: Molecular and Polymer Gels and Materials with Self-Assembled Fibrillar Networks special issue.

(1) (a) Terech, P.; Weiss, R. G. *Chem. Rev.* **1997**, *97*, 3133–3159. (b) Shinkai, S.; Murata, K. *J. Mater. Chem.* **1998**, *8*, 485–495. (c) Abdallah, D. J.; Weiss, R. G. *Adv. Mater.* **2000**, *12*, 1237–1247. (d) van Esch, J. H.; Feringa, B. L. *Angew. Chem., Int. Ed.* **2000**, *39*, 2263–2266. (e) Sangeetha, N. M.; Maitra, U. *Chem. Soc. Rev.* **2005**, *34*, 821–836. (f) Weiss, R. G., Terech, P., Eds. *Molecular Gels. Materials with Self-Assembled Fibrillar Networks*; Springer: Dordrecht, The Netherlands, **2006**. (g) George, M.; Weiss, R. G. *Acc. Chem. Res.* **2006**, *39*, 489–497.

(2) van Esch, J. H.; Schoonbeek, F.; Loos, M. D.; Veen, E. M.; Kellog, R. M.; Feringa, B. L. In *Supramolecular Science: Where It Is and Where It Is Going*; Ungar, R., Dalcanale, E., Eds.; Kluwer Academic Publishers: The Netherlands, **1999**; pp 233–259.

(3) Srivastava, S. P.; Saxena, A. K.; Tandon, R. S.; Shekher, V. *Fuel* **1997**, *76*, 625–630.

(4) Abdallah, D. J.; Weiss, R. G. *Langmuir* **2000**, *16*, 352–355.

(5) Abdallah, D. J.; Sirchio, S. A.; Weiss, R. G. *Langmuir* **2000**, *16*, 7558–7561.

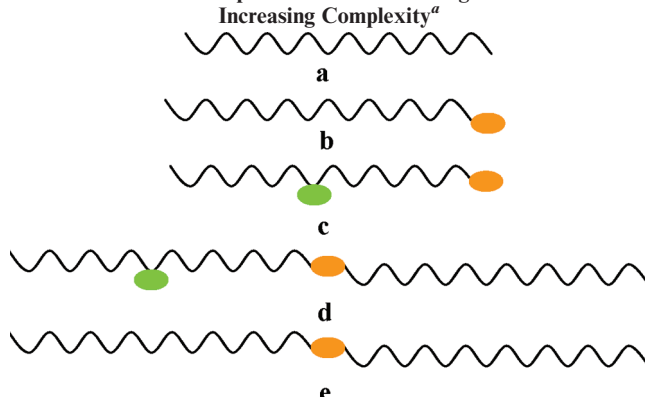
(6) (a) George, M.; Weiss, R. G. *J. Am. Chem. Soc.* **2001**, *123*, 10393–10394. (b) Ballabh, A.; Trivedi, D. R.; Dastidar, P. *Chem. Mater.* **2006**, *18*, 3795–3800.

(7) (a) Marton, L.; McBain, J. W.; Vold, R. D. *J. Am. Chem. Soc.* **1941**, *63*, 1990–1993. (b) Zana, R. *Langmuir* **2004**, *20*, 5666–5668. (c) Novales, B.; Navilles, L.; Axelos, M.; Nallet, I.; Douliez, J.-P. *Langmuir* **2008**, *24*, 62–68.

(8) Mieden-Gundert, G.; Klein, L.; Fischer, M.; Vogtle, F.; Heuze, K.; Pozzo, J.-L.; Vallier, M.; Fages, F. *Angew. Chem., Int. Ed.* **2001**, *40*, 3164–3166.

(9) Gaspar, L. J. M.; Baskar, G. *J. Mater. Chem.* **2005**, *15*, 5144–5150.

(10) Lescanne, M.; Grondin, P.; D'Aleo, A.; Fages, F.; Pozzo, J.-L.; Monval, O. M.; Reinheimer, P.; Collin, A. *Langmuir* **2004**, *20*, 3032–3041.

Scheme 1. Cartoon Representation of the Design of LMOGs with Increasing Complexity^a

^a Starting from (a) an *n*-alkane gelator and changing to (b) an *n*-alkane with a terminal functional group (orange oval), (c) an *n*-alkane with a terminal and an “interior” pendant functional group (green oval), (d) an *n*-alkane with two functional groups, including an alkyl chain on the terminal functionality, and (e) an *n*-alkane with terminal functionality to which an alkyl group has been appended.

occurring carboxylic acid (available from castor oil¹¹), 12-hydroxystearic acid (**HSA**; i.e., 12-hydroxyoctadecanoic acid (Figure 1)),¹² which is easily obtained as its (*R*) enantiomer. Enantiopure **HSA** exhibits circular dichroic signals that are attributed to helical arrangements of the molecules in their fibrillar networks.^{12d,12e} Previous reports showed that alkali metal salts of **HSA** have twisted fibrous networks in their gel state.^{12f–12i}

The link between the molecular structure of a gelator and either its efficiency in constructing the self-assembled fibrillar networks (**SAFINs**) of gels or the nature of those **SAFINs** is not obvious.¹³ Many **LMOGs** are polymorphous, and it is known that small changes in molecular structure can lead to large changes in crystal packing. For example, primary amides generally form tape-like structures whereas secondary amides form chainlike structures;¹⁴ urea is able to form clathrates in the presence of long *n*-alkanes, but *N,N'*-dimethylurea as small as *N,N'*-dimethylurea organize into fibers and **SAFINs**, leading to gels.¹⁵ Thus, it is important to investigate the relationship between molecular structure and gelation properties in a series of molecules that differ structurally in a rational way.

Such an investigation is presented here for molecules of the **c**- and **d**-types in Scheme 1 using **HSA** as the base structure. Also, comparisons are made with gels containing **LMOGs** derived from **SA** (i.e., **b**- and **e**-type molecules that are analogs of **HSA** in which the 12-hydroxyl group has been removed).

(11) Maskaev, A. K.; Man'kovskaya, N. K.; Lend'el, I. V.; Fedorovskii, V. T.; Simurova, E. I.; Terent'eva, V. N. *Chem. Technol. Fuels Oils* **1971**, *7*, 109–112.

(12) (a) Terech, P.; Rodriguez, V.; Barnes, J. D.; McKenna, G. B. *Langmuir* **1994**, *10*, 3406–3418. (b) Terech, P.; Pasquier, D.; Bordas, V.; Rossat, C. *Langmuir* **2000**, *16*, 4485–4494. (c) Tsau, J. S.; Heller, J. P.; Pratap, G. *Polym. Prepr.* **1994**, *35*, 737–738. (d) Tachibana, T.; Mori, T.; Hori, K. *Bull. Chem. Soc. Jpn.* **1980**, *53*, 1714–1719. (e) Tachibana, T.; Mori, T.; Hori, K. *Bull. Chem. Soc. Jpn.* **1981**, *54*, 73–80. (f) Tachibana, T.; Kitazawa, S.; Takeno, H. *Bull. Chem. Soc. Jpn.* **1970**, *43*, 2418–2421. (g) Tachibana, T.; Kambara, H. *Bull. Chem. Soc. Jpn.* **1969**, *42*, 3422–3424. (h) Tachibana, T.; Kambara, H. *J. Am. Chem. Soc.* **1965**, *87*, 3015–3016. (i) Terech, P. *Colloid Polym. Sci.* **1991**, *269*, 490–500.

(13) George, M.; Weiss, R. G. In *Molecular Gels. Materials with Self-Assembled Fibrillar Networks*; Weiss, R. G.; Terech, P., Eds.; Springer: Dordrecht, The Netherlands, **2006**; pp 449–551.

(14) Burrows, A. D. In *Structure and Bonding*; Mingos, D. M. P., Ed.; Springer-Verlag: Berlin, **2004**; Vol. 108, pp 55–96.

(15) George, M.; Tan, G.; John, V. T.; Weiss, R. G. *Chem.—Eur. J.* **2005**, *11*, 3243–3255.

We explore how the gelating properties are affected when the terminal functional group of **HSA** is modified systematically by introducing nitrogen-containing moieties. Those data, and the complementary information from the **SA** analogs, are used to identify the factors that appear to be most important in generating very efficient **LMOGs** of molecules with long alkyl chains as their primary structural unit. The specific derivatives of **HSA** explored here are amides **1–6** and amines **7–12** and the ammonium carbamate salt of **7**, compound **13**. The underlying concepts behind the choice of these molecules are that H bonding between amides can be stronger than between amines and that the *N*-alkyl groups and charged centers at the head groups of **13** can modify the molecular packing of the **LMOGs** within their fibrillar aggregates. The availability of gelation data from the parent molecule, **HSA**, and from several nitrogen-containing derivatives of the corresponding acid without a hydroxyl moiety, **SA** (**b**- and **e**-type gelators in Scheme 1), allows interesting structure–gelation correlations to be derived.

The data demonstrate that the introduction of a 12-hydroxyl group and the presence of a primary amide group increase the efficiency of the gelators. This assessment is based upon gelation temperatures, temporal stabilities (the time between when gels were prepared in sealed containers at ~24 °C and when they undergo visual phase separation or flow when inverted), critical gelator concentrations (CGCs; the lowest concentrations of **LMOG** at which a gel is formed at room temperature), and ranges of liquids gelated. The stabilities of the gels are then correlated with the structures of the **LMOGs** and their **SAFINs**. Furthermore, some of the gels exhibit exceedingly fast and high degrees of recovery of their viscoelastic properties after their shear-induced destruction; they are thixotropic. Although fast recovery of viscoelasticity has been found in hydrogels where the **SAFIN** is composed of amorphous objects,¹⁶ we are not aware of other examples in which the fibrillar objects are crystalline and the liquids are organic, as they are here.

Experimental Section

Details concerning the preparation, purification, and characterization of the **LMOGs** are collected in the Supporting Information file.

Instrumentation and Procedures. ¹H-NMR spectra were recorded on a Varian 300 MHz spectrometer interfaced to a Sparc UNIX computer using Mercury software. Chemical shifts were referenced to an internal standard, tetramethylsilane (TMS). IR spectra were obtained on a Perkin-Elmer Spectrum One FTIR spectrometer interfaced to a personal computer. Elemental analyses were performed on a Perkin-Elmer 2400 CHN elemental analyzer using acetanilide as a calibration standard. Melting points and optical micrographs (POMs) were recorded on a Leitz 585 SM-LUX-POL microscope equipped with crossed polars, a Leitz 350 heating stage, a Photometrics CCD camera interfaced to a computer, and an Omega HH503 micropressure thermometer connected to a J-K-T thermocouple. The samples for POM were flame sealed in 0.4 or 0.5 mm path-length, flattened Pyrex capillary tubes (VitroCom) heated to their liquid phase in a boiling water bath and cooled accord-

(16) (a) Nowak, A. P.; Breedveld, V.; Pakstis, L.; Ozbas, B.; Pine, D. J.; Pochan, D.; Deming, T. J. *Nature* **2002**, *417*, 424–428. (b) Zhang, S.; Holmes, T.; Lockshin, C.; Rich, A. *Proc. Natl. Acad. Sci. U.S.A.* **1993**, *90*, 3334–3338. (c) Ramachandran, S.; Tseng, Y.; Yu, Y. B. *Biomacromolecules* **2005**, *6*, 1316–1321. (d) Xu, J.; Liu, Z. S.; Erhan, S. Z. *J. Am. Oil Chem. Soc.* **2008**, *85*, 285–290. (e) Kundu, S. K.; Matsunaga, T.; Yoshida, M.; Shibayama, M. *J. Phys. Chem. B* **2008**, *112*, 11537–11541.

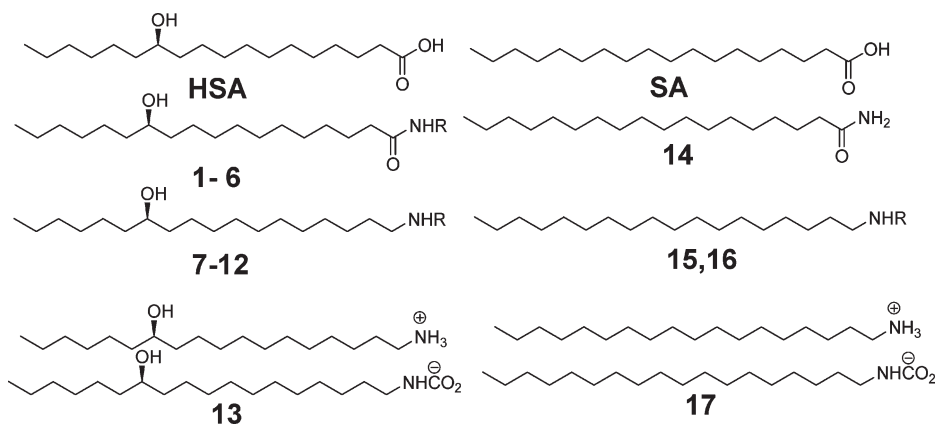


Figure 1. Structures of LMOGs derived from **HSA** and those lacking a hydroxyl group from **SA** upon which comparisons are made for **1**, **7**, and **15** ($R = H$); for **2** and **8** ($R = CH_3$); for **3** and **9** ($R = C_2H_5$); for **4** and **10** ($R = C_3H_7$); for **5** and **11** ($R = C_4H_9$); for **6**, **12**, and **16** ($R = C_{18}H_{37}$); and for **13** and **17**.

ing to protocols described below. Powder X-ray diffraction (XRD) patterns of samples were obtained on a Rigaku R-AXIS image plate system with $Cu K\alpha$ X-rays ($\lambda = 1.54 \text{ \AA}$) generated by a Rigaku generator operating at 46 kV and 40 mA with the collimator at 0.5 mm (to obtain 0.5-mm-diameter beams of X-rays¹⁷). Data processing and analyses were performed using Materials Data JADE (version 5.0.35) XRD pattern processing software. Samples were sealed in 0.5 mm glass capillaries (W. Müller, Schönwalde, Germany), and diffraction data were collected for 2 (neat powders) or 10 h (gels). Differential scanning calorimetry (DSC) and thermogravimetric analyses (TGA) were performed on a TA 2910 differential scanning calorimeter interfaced to a TA Thermal Analyst 3100 controller under a slow stream of nitrogen flowing through the cell. Samples were in closed aluminum pans for DSC and in open ones for TGA measurements. Transition temperatures from DSC (T_m) are reported at the onsets of endotherms (on heating) and exotherms (on cooling). Heating rates were $5 \text{ }^{\circ}\text{C}/\text{min}$; cooling rates were variable and depended on the difference between the cell block and ambient temperature. Rheological measurements were obtained on an Anton Paar Physica MCR 301 rheometer using Peltier-controlled parallel plates (25 mm diameter). The gap between the parallel plates was 0.5 mm unless indicated otherwise, and the data were collected using Rheoplus/32 Service V3.10 software. Before data were recorded, each sample was placed between the shearing plates of the rheometer and heated to $120 \text{ }^{\circ}\text{C}$ to ensure that a solution/sol was present. It was cooled to $10 \text{ }^{\circ}\text{C}$ (at $\sim 20 \text{ }^{\circ}\text{C min}^{-1}$), the temperature was increased to $25 \text{ }^{\circ}\text{C}$, and the sample was incubated there for 15 min to reform the gel and remove any shear-induced alignment of the fibers of **SAFIN**.

Scanning electron microscopy (SEM) images were recorded with 2–30 kV electron beam energies on a Zeiss Supra 55 VP electron scanning microscope. Samples for SEM were prepared by placing the gel sample on an Al mount (1/200 slotted head, 1/800 pin, Ted Pella, Inc.) and allowing the solvent to evaporate at $24 \text{ }^{\circ}\text{C}$ for 24 h. No metal coating was applied.

Fast and Slow Cooling Procedures for the Preparation of Gels from Sols and Analyses of Gels. Fast-cooled gels were prepared by placing weighed amounts of a liquid and gelator into a glass tube (5 mm i.d.) that was then flame-sealed. The mixture was heated to ca. $80 \text{ }^{\circ}\text{C}$ in a water bath (or to $110 \text{ }^{\circ}\text{C}$ in an oil bath with **1**) until a solution/sol was obtained and was then placed directly into an ice–water bath for 10 min. After the sample was warmed to room temperature for 1 h, its appearance was noted. Slow-cooled gels were prepared using the protocol

above except that the hot solutions/sols were kept in the water or oil bath while they returned slowly to room temperature.

Temperatures of Gelation and Critical Gelation Concentrations (CGC). Gelation temperatures (T_g) were determined by the inverse flow method¹⁸ (i.e., the temperature ranges over which a gel fell under the influence of gravity when inverted in a sealed glass tube that was placed in a water bath that was heated from room temperature at ca. $1.5 \text{ }^{\circ}\text{C min}^{-1}$). CGCs were determined from a series of fast-cooled gels with different LMOG concentrations; the concentration of the one with the lowest gelator concentration that did not fall when inverted at $24 \text{ }^{\circ}\text{C}$ is reported.

Results and Discussion

Gelation Studies: General Aspects. The gelation properties of 2 wt % **HSA** and **1–13** in a wide range of liquids are summarized in Tables 1 and 2. Because many of the liquids are volatile and some evaporation from their samples can occur when they are not in hermetically sealed containers, many of our studies have employed gels with a very low volatility liquid, silicone oil (tetramethyltetraphenylsiloxane).

SAFIN structures of **HSA** organogels have been studied extensively.^{12a} Head-to-head contacts between carboxylic acid groups have been shown to promote the formation of multiple hydrogen-bonded sequences and aid fiber stability. The T_g values of 2 wt % **HSA** and an *n*-alkane with an even number of carbon atoms are slightly higher than those with odd-numbered *n*-alkane liquids, but all were opaque in appearance. The dependence of the **SAFINs** of the **HSA** gels on the liquid component is apparent when silicone oil and *n*-alkanes are compared: at one LMOG concentration, the silicone oil gel has a higher T_g than the *n*-alkane gels. Also, the sodium salt of **HSA** has been found to gelate *n*-dodecane at 4 wt %, and as little as 0.5 wt % was able to gelate chloroform and carbon tetrachloride.²⁰

Intermolecular H-bonding interactions between primary or secondary amide functional groups can be stronger than between two carboxylic acid groups.²¹ Thus, the T_g of

(18) Takahashi, A.; Sakai, M.; Kato, T. *Polym. J.* **1980**, *12*, 335–341.

(19) The transition between the opaque and clear gel states is reversible and first order according to DSC thermograms. Additional data and more detailed analyses will be reported in the future.

(20) Huang, X.; Weiss, R. G. *Tetrahedron* **2007**, *63*, 7375–7385.

(21) Scheiner, , S. *Hydrogen Bonding: A Theoretical Perspective*; Oxford University Press: New York, **1997**; p 121.

Table 1. Appearances,^a T_g Values (°C), and Periods of Stability^b (in Parentheses) of Gels Containing 2 wt % HSA and Its Amide Derivatives (1–6) in Various Liquids

liquid	HSA	1	2	3	4	5	6
<i>n</i> -hexane	OG (59–60, 2 m)	OG (syn, 91–92, ^c 4 m)	OG (syn, 82–83, > 3 w)	OG (syn, 81, ^c > 1 m)	OG (syn, 82, ^c 2 m)	OG (syn, 74–75, ^c > 1 m)	OG (syn, 78, ^c 2 m)
<i>n</i> -octane	OG (60–62, > 9 m ^d)	OG (94–95, ^c 4 m)	OG (84–85, ^c > 3 w)	OG (84, ^c > 1 m)	OG (syn, > 90, ^c 5 m)	OG (74, ^c > 1 m)	OG (syn, 81, ^c 2 m)
<i>n</i> -decane	OG (64–65, > 9 m)	OG (95–96, ^c > 1 y)	OG c > 3 w)	OG (89–90, ^c > 1 m)	OG (syn, > 90, ^c > 1 y)	P	OG (syn, 83, ^c > 1 y)
silicone oil	OG (73–74, > 9 m)	OG (98–100, > 1 y)	OG (90–91, > 3 w)	OG (86–87, > 1 m)	OG (83–85, > 1 y)	OG (82–84, > 1 m)	OG (83–84, > 1 y)
methanol	soln	soln	P	soln	soln	soln	P
1-butanol	soln	soln	soln	soln	soln	P	visc soln
1-octanol	soln	OG (syn, 27–34, > 1 y)	P	P	soln	P	visc soln
benzyl alcohol	soln	soln	soln	soln	soln	soln	visc soln
chlorobenzene	CG (46–48, > 9 m)	CG (63–64, > 1 y)	OG (56–57, > 3 w)	OG (49–50, > 1 m)	OG (52, > 1 y)	OG (46, > 1 m)	OG (55–57, > 1 y) ^e
chloroform	OG (21–22)	OG (syn, 38, 4 m)	P	soln	soln	soln	P
CCl ₄	CG (syn, 41, > 9 m)	OG (syn, 63, ^c 4 m)	OG (syn, 68–69, > 3 w)	OG (syn, 64–66, > 1 m)	OG (syn, 58–60, 2 d)	OG (syn, 59–60, > 1 m)	OG + visc soln
<i>n</i> -perfluoroctane	I	I	I	I	I	I	I
benzene	CG (49–50, 5 m)	CG (64–65, 7 m ^d)	OG (58–60, > 3 w)	OG (57–61, > 1 m)	OG (54–55, 2 m)	OG (47, > 1 m)	P
toluene	CG (44–45, 9 m ^d)	CG (65–67, > 1 y ^e)	OG (61–62, > 3 w)	OG (57–58, > 1 m)	OG (55–58, > 1 y ^e)	OG (syn, 51, > 1 m)	OG (syn, 58, 5 m)
DMSO	soln	soln	OG (45–47, > 3 w)	OG (44–47, > 1 m)	OG (52, > 1 y)	OG (55–56, > 1 m)	OG (syn, 74–75, 2 d)
acetonitrile	OG (45–48, 2 m)	OG (53–54, 2 m)	OG (59–60, ^c > 3 w)	OG (56, ^c > 1 m)	OG (62, 2 m)	OG (55, ^c > 1 m)	P
water	I	I	I	I	I	I	I

^a OG - opaque gel, syn - syneresis, soln - solution, visc - viscous, P - precipitate, I - insoluble, CG - clear gel, y - year, m - month, d - day, w - week. ^b The periods of stability were measured as the time between when gels were prepared in sealed containers at ~24 °C and when they underwent phase separation that could be detected visually; temporal stabilities of gels with T_g below 24 °C were not measured. ^c Phase separation: liquid fell upon heating; some or all solid did not. ^d Syneresis after 2 months. ^e Syneresis after 8 months.

Table 2. Appearances,^a T_g Values (°C), and Periods of Stability^b (in Parentheses) of Gels Containing 2 wt % Amine Derivatives of HSA (7–12) and the Ammonium Carbamate Salt of 7 (13) in Various Liquids

liquid	7	8	9	10	11	12	13
<i>n</i> -hexane	P	P	P	OG (syn, 40–41, 2 d)	P	P	P
<i>n</i> -octane	P	P	P	OG (syn, 46, 1 w)	P	P	P
<i>n</i> -decane	P	P	P	OG (49, 1 m)	P	P	P
silicone oil	OG (21–22)	OG (55–56, > 1 m)	OG (57–58, > 3 w)	OG (62–63, > 1 y)	OG (62–64, > 1 m)	OG (67–69, > 1 y)	OG (0–2)
methanol	soln	soln	soln	P	soln	P	P
1-butanol	soln	soln	soln	soln	soln	visc soln	P
1-octanol	soln	P	soln	soln	soln	visc soln	visc soln
benzyl alcohol	soln	soln	soln	soln	soln	soln + P	P
chlorobenzene	soln	visc soln	visc soln	visc soln	soln	P	OG (54–55, 5 m)
chloroform	CG (syn, 34–35, 4 m)	soln	soln	soln	soln	visc soln	OG (syn, 39–40, > 1 y)
CCl ₄	visc soln	TG (> 1 m)	OG (syn, 69–70, ^c > 1 m)	OG (74–75, ^c > 1 y)	TG (72–74, > 1 m)	visc soln	soln
<i>n</i> -perfluoroctane	I	I	I	I	I	I	I
benzene	soln	soln	P	soln	P	P	P
toluene	visc soln	soln	soln	OG (syn, 33–35, 1 h)	soln	P	soln
DMSO	visc soln	OG (36–42, > 3 w)	OG (syn, 33–36, > 1 m)	OG (59–60, 2 m)	OG (55–56, > 2 m)	OG (63–83, 2 m)	soln
acetonitrile	P	P	P	P	P	P	P
water	I	I	I	I	I	I	I

^a OG - opaque gel, syn - syneresis, soln - solution, visc - viscous, P - precipitate, I - insoluble, TG - translucent gel, CG - clear gel, y - year, m - month, d - day, w - week. ^b The periods of stability were measured as the time between when gels were prepared in sealed containers at ~24 °C and when they underwent phase separation that could be detected visually; temporal stabilities of gels with T_g below 24 °C were not measured. ^c Transformed to a CG at 35 °C.¹⁹

n-alkane or silicone oil gels is higher when the **LMOG** was one of the amides, **1–6**, than when it was **HSA**. Removal of the 12-hydroxyl group from **1** yields octadecanamide (**14**), which, in contrast to **SA**, is an excellent gelator. However, whereas 2 wt % **1** is a better gelator of lower-polarity liquids and forms solutions with low molecular-mass alcohols, the same concentration of **14** is a more efficient **LMOG** of higher-polarity liquids and precipitates from *n*-alkanes (Supporting Information file, Table S1). For example, the T_g values for 2 wt % **14** gels are lower than those of **1** in silicone oil, benzene, and toluene but are higher in acetonitrile; in DMSO, **1** is dissolved whereas **14** forms a stable gel. This contrasting behavior, caused by the presence or absence of a 12-hydroxyl group along the long alkyl chain, can be traced to the relative solubilities of the two **LMOGs**: **14** is more soluble in less-polar liquids, and **1** is more soluble in more-polar liquids.

The addition of an alkyl group to the amide group of **1** has two effects on its ability to gelate liquids: (1) the amides lose some of their potential to create H-bonding networks because one of the H atoms is replaced; (2) the amide group is moved from a molecular terminus to an interior position. The general trend in Table 1 toward lower T_g values in liquids such as silicone oil, CCl_4 , chlorobenzene, benzene, and toluene as the amide functional group of the **LMOG** is moved farther from a terminus (i.e., $T_g(\mathbf{1}) > T_g(\mathbf{2}) > T_g(\mathbf{3})$) must be interpreted with caution; at constant amide wt %, the molar concentrations decrease as the length of the alkyl group increases and the number of possible H-bonding and London dispersive interactions decreases and increases, respectively. Possible changes in the molecular packing arrangements within a fiber (vide infra) add other complications. In addition, because the CGCs differ in each liquid, the total amount of an **LMOG** participating in the **SAFIN** of a gel will also differ, and the variation will not be constant from gelator to gelator.

Figure 2 shows the T_g values versus alkyl chain length for the gels of **1–6** in different liquids. Except for DMSO gels, the T_g values for the primary amide (**1**) were higher than those of the secondary amides with *N*-methyl or *N*-ethyl groups (**2** or **3**), but further increases in the *N*-alkyl chain length do not appreciably alter the T_g values. DMSO gels of **1–6** behaved differently: $T_g(\mathbf{6}) > T_g(\mathbf{5}) > T_g(\mathbf{4})$ and 2 wt % **1** remained soluble in DMSO at room temperature. Again, this trend appears to be related to the solubilities of the amides in DMSO, and there is a precedent for such behavior in other gel systems.²²

H-bonding between amine groups is generally weaker than between amides, and as mentioned above, the differences between amino–amino and amido–amido aggregation modes may lead to changes in the overall packing arrangements of the gelator molecules in their fibers.¹ The importance of the stronger amide–amide interactions in the stabilization of the **SAFINs** is evident when the gels employing the amides (**1–6**) and the analogous amines (**7–12**) are compared. For example, the primary amine (**7**) is a much less efficient gelator than its primary amide analogue, **1**; it gelates fewer of the investigated liquids, and its gels exhibit lower T_g values. Interestingly, **7** is also a much less efficient gelator

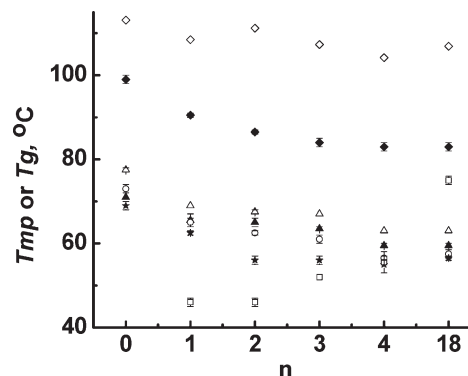


Figure 2. Plots of the melting points (T_{mp}) of the neat amide gelators (**1–6**) (\diamond) or the T_g values of their gels with various liquids versus n , the number of carbon atoms in their *N*-alkyl chains: 2 wt % gel in silicone oil (\blacklozenge), 5 wt % gel in CCl_4 (Δ), 5 wt % gel in benzene (\square), 5 wt % gel in toluene (\blacktriangle), 5 wt % gel in chlorobenzene (\star), and 2 wt % gel in DMSO (\blacksquare). Temperature ranges of vertical bars indicate when the initial and final portions of an inverted gel sample fell on being heated slowly.

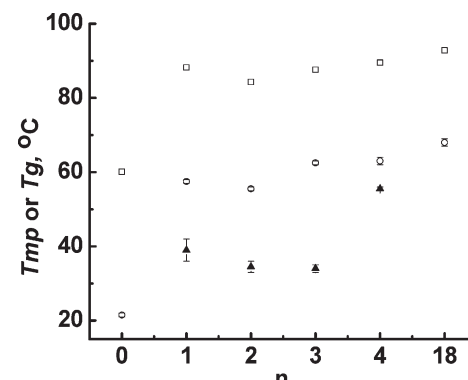


Figure 3. Plots of the melting points (T_{mp}) of the neat amine gelators (**7–12**) (\square) or the T_g values of their gels with various liquids versus n , the number of carbon atoms in their *N*-alkyl chains: 2 wt % gel in silicone oil (\circ) and 2 wt % gel in DMSO (\blacktriangle). Temperature ranges of vertical bars refer to when the initial and final portions of a gel sample fell on being heated slowly; the absence of a space bar indicates that the range was smaller than the symbol.

than the secondary amine, **8**, in which a methyl group replaces one of the H atoms on nitrogen (and thereby eliminates one potential H-bonding interaction). Figure 3 presents a comparison of T_g values of the gels of **7–12** in DMSO and silicone oil. The trends in the silicone oil gels correlate with the melting temperatures of the neat gelators. This correlation and the very small temperature ranges for the gels indicate that the thermodynamic driving force for supersaturated solutions/sols in silicone oil is very large and that the gelator molecules are able to aggregate and nucleate rapidly below T_g . Whereas 2 wt % **7** is a viscous solution in DMSO at room temperature, 2 wt % **8** forms an opaque gel. The highest T_g value of the amine **LMOGs** investigated was found for the *N*-butyl derivative (**11**), and 2 wt % **12** in DMSO formed a precipitate when cooled from its sol phase.

1-Octadecylamine (**15**), the analogue of **7** lacking a 12-hydroxy group, is known to gelate silicone oil and DMSO at 5 wt %, and di-*n*-octadecyl amine (**18**), the corresponding analogue of secondary amine **12**, forms gels with alkanes and alcohols (among other liquids), albeit with low T_g values

(22) (a) Hirst, A. R.; Coates, I. A.; Boucheteau, T. R.; Miravet, J. F.; Escuder, B.; Castelletto, V.; Hamley, I. W.; Smith, D. K. *J. Am. Chem. Soc.* **2008**, *130*, 9113–9121. (b) Mukkamala, R.; Weiss, R. G. *Langmuir* **1996**, *12*, 1474–1482. (c) Lu, L.; Cocker, T. M.; Bachman, R. E.; Weiss, R. G. *Langmuir* **2000**, *16*, 20–34.

(Supporting Information file, Table S1).²³ Thus, the removal of the hydroxyl group (and its H-bonding interactions) from **7** or **12** reduces the gelating abilities further.

Ammonium carbamate (**13**), prepared by the addition of CO₂ to 1-aminoctadecan-12-ol (**7**),^{6a} is a less-efficient LMOG than any of **1–12** or **HSA**. For example, the T_g values of silicone oil gels with 2 wt % gelator increase in the order **13** (0–2 °C) < **7** < **HSA**. To effect self-assembly, molecules of **13** must rely principally upon electrostatic interactions of the head groups and H-bonding among 12-hydroxyl groups; London dispersion forces among methylene units along the chains contribute as well.^{1c,1g} Thus, it is somewhat surprising, given the comparisons of the gelating abilities of **7** and **12** and their nonhydroxylated analogues (**15** and **16**), that **13** is a less efficient gelator than even the ammonium carbamate (**17**), which gels silicone oil, benzyl alcohol, toluene, and DMSO (Supporting Information file, Table S1).²⁴ However, we note that the T_g of the gel from 2 wt % **13** in chlorobenzene is higher than that from even **HSA**, and **7** yielded no gel. Clearly, any correlation between LMOG structure and gelator efficiency must take into consideration some very complicated bulk and molecular aspects of interactions with the liquid components.

Dependence of Gel Properties on LMOG Concentration.

The data in Figure 4 show that ≤1 wt % of each of the LMOGs included, except **7** and **13**, is able to gelate silicone oil at room temperature. A clear gel was formed at room temperature even at 0.06 wt % **1**, and the T_g values of these gels in the “plateau” concentration region (ca. 2–5 wt %, where the 3D SAFINs become more intricate but their basic structures and interactions are not changed appreciably^{1f}) are very high, near 100 °C. At room temperature, the gels remained clear to concentrations ≤0.5 wt % and became increasingly opaque thereafter up to 5 wt %.

Silicone oil gels of the *N*-propyl amide (**4**) and *N*-octadecyl amide (**6**) are opaque throughout the concentration ranges explored. Although both are exceedingly effective gelators, their CGCs are slightly higher (0.2 and 0.4 wt %, respectively) than that of **1**. The consequences of weaker H-bonding between amino groups of amine gelators **7**, **10**, and **12** are evident in both their CGC and T_g values; the CGC values are higher and the T_g values are lower than for the corresponding amides.

Table 3 summarizes the CGCs, appearances, and stability periods of silicone oil and toluene gels of **1**, **4**, **6**, **7**, **10**, and **12** at room temperature. These data consistently show that less LMOG is necessary to form a gel in silicone oil than in toluene because the LMOGs are more soluble in the latter, but there is no clear trend in the dependence of the liquid on periods of stability. The concentration dependence of **1** and **4** on the gelation properties in toluene has also been examined (Supporting Information file, Figure S3): gels using 0.2–2.0 wt % **1** were clear, and 3–5 wt % gels were opaque in appearance; gels with 0.3–5.0 wt % **4** were transparent.

In some systems, including those in which *N,N'*-dialkyl ureas are the LMOGs,¹⁵ the cooling protocol can lead to very different SAFINs with different T_g values.^{23,25,26} That does

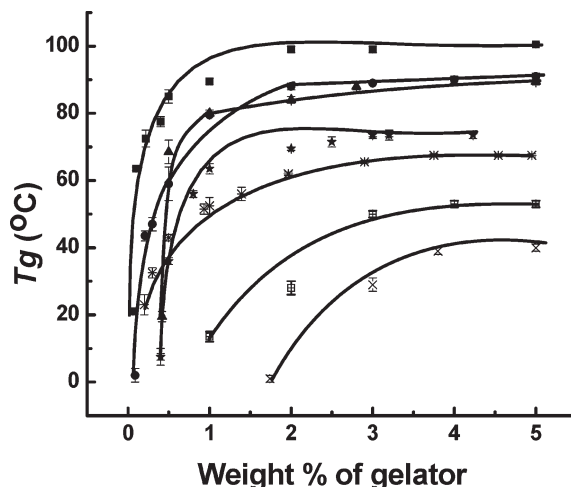


Figure 4. T_g values of silicone oil gels as a function of concentration of **1** (■), **4** (●), **6** (▲), **7** (■), **10** (*), **12** (★), and **13** (×). The lines have no physical meaning; they are included to observe trends. Temperature ranges of vertical bars refer to when the initial and final portions of a gel sample fell on being heated slowly.

Table 3. CGCs (wt %), Appearance (AP),^a and Periods of Stability (PS)^b for Silicone Oil and Toluene Gels with LMOGs **1, **4**, **6**, **7**, **10**, and **12** Prepared Using the Fast-Cooling Protocol**

	silicone oil			toluene		
	CGC	AP	PS	CGC	AP	PS
1	0.1	CG	4 d	0.3	CG	2 m ^c
4	0.2	CG	2 m ^d	0.3	CG	2 m ^c
6	0.4	OG	16 h ^c	2.0	OG (syn)	5 m
7	2.0 ^e	OG ^e		no gel		
10	0.2	OG	2 w	2.0	OG	1 h
12	0.5	OG	18 h	no gel		

^a OG - opaque gel, CG - clear gel, syn - syneresis. ^b Periods at ~24 °C in sealed containers between when gels were prepared and when visible phase separation was noted; m - month, d - day, w - week. ^c Syneresis after 1 h. ^d Syneresis after 2 weeks. ^e T_g = 21–22 °C; temporal stabilities of gels with T_g below 24 °C were not measured.

not appear to be the case here. The gelation temperatures of the **HSA** derivatives in silicone oil were compared when their gels (at low and high LMOG concentrations) were prepared from their sols by fast- and slow-cooling protocols. (Supporting Information file, Table S2). The T_g values were not sensitive to the cooling protocol except for the gel with 0.42 wt % **6**, where T_g = 21–23 and 73–74 °C for gels made by the fast- and slow-cooling protocols, respectively. The reason for this large change appears to be related to a change in the morphology of its SAFIN (vide infra).

The mean temperature at which a SAFIN melts, T_m , and the heat associated with that transition have been measured by DSC for silicone oil gels at relatively high LMOG concentrations (in order to observe the endothermic and exothermic peaks easily in the thermograms). The normalized enthalpies (per gram of LMOG; see Table 4) as well as the entropies ($\Delta S = \Delta H/T_m$) of the reversible transitions were calculated using the averages of the absolute magnitudes of ΔH and the onset temperatures from the first heating and cooling thermograms of the silicone oil gels and neat solids. As expected, the T_m values of the SAFINs are always lower than the melting temperatures of the neat LMOGs; the silicone oil liquid aids SAFIN melting by

(23) Abdallah, D. J.; Lu, L.; Weiss, R. G. *Chem. Mater.* **1999**, *11*, 2907–2911.

(24) George, M.; Weiss, R. G. *Langmuir* **2002**, *18*, 7124–7135.

(25) (a) Lin, Y.; Kachar, B.; Weiss, R. G. *J. Am. Chem. Soc.* **1989**, *111*, 5542–5551. (b) Furman, I.; Weiss, R. G. *Langmuir* **1993**, *9*, 2084–2088.

(26) Abdallah, D. J.; Weiss, R. G. *Chem. Mater.* **2002**, *14*, 406–413.

Table 4. Comparison of T_m , ΔH ,^a and ΔS of Silicone Oil Gels and Neat Solids of 1, 4, 6, 8, and 12 during Their First Heating and Cooling, from DSC Thermograms, and T_g Values from the Falling Drop Method

gelator	conc	heating		cooling		T_g (°C)	ΔS (J mol ⁻¹ K ⁻¹)
		T_m (°C)	ΔH (kJ mol ⁻¹)	T_m (°C)	$-\Delta H$ (kJ mol ⁻¹)		
1	4.6 wt %	100.1	51.8 ^b	104.6	48.5 ^b	100	134
	neat	113.4	49.4	111.2	48.8		127
4	5.2 wt %	94.3	49.5 ^c	90.0	47.5 ^c	90–92	133
	neat	107.5	55.0	101.5	53.6		144
6	5.0 wt %	91.7	86.1 ^d	91.7	71.2 ^d	89–90	216
	neat	106.8	94.4	104.0	81.1		232
8	4.8 wt %	59.1	50.7 ^e	60.7	43.9 ^e	67–68	142
	neat	87.6	67.4	83.8	65.5		185
12	4.8 wt %	73.1	83.4 ^e	70.9	70.5 ^e	74–76	223
	neat	93.1	95.8	87.8	95.8		263

^a ΔH values from the gels are normalized to 100% concentrations of the **LMOG** component by dividing the observed heats by the quantities listed in footnotes b–e. ^b 0.046. ^c 0.052. ^d 0.05. ^e 0.048.

dissolving the molecules in the fibers over a temperature range that precedes the loss of viscoelasticity.

Thus, the normalized heats of the gel transitions are generally lower than those of the associated neat **LMOG**. Only with the most efficient **LMOG** (**1**) do the normalized heats of the gels approach the heats found for the neat solid. In all other cases, the enthalpy and entropy values indicate that the dissolution of the **LMOGs** as their **SAFINs** melt is aided somewhat by silicone oil. In addition, the similarity between the T_m and T_g values in Table 4 indicates that the loss of the viscoelastic properties of these gels occurs as the bulk of the **LMOG** molecules melt, rather than at an earlier possible stage (e.g., when the junction zones between the fibers of **SAFIN** are severed).^{1a,13}

SAFIN Structural Information from Polarizing Optical Microscopy and Scanning Electron Microscopy. As has been found in many other systems, the spherulites of gels from the **HSA** derivatives are larger when prepared by the slow-cooling protocol; see, for example, the POMs in Figure 5. Generally, more supersaturation results in smaller and more numerous crystals,²⁷ and the driving force for the phase separation of a sol, leading to nucleation, fiber growth, and **SAFIN** formation, increases with increasing supersaturation (i.e., as the reduced gelation temperature, $T_g - T$, for sol incubation increases)²⁸ whereas the sizes of the basic **SAFIN** units (fibers or spherulites) decrease and become more numerous or the morphology of the **LMOG** objects changes.^{25,29}

The spherulitic objects of slow-cooled gels of 2 wt % **4** in *n*-decane, CCl_4 , DMSO, or silicone oil are larger than from the fast-cooled ones (Supporting Information file, Figures S4–S8). The fast-cooled gels of **4** in toluene and the 2 wt % gels of **6**, **10**, and **12** show spherulitic textures similar to those of **1** in Figure 5c (Supporting Information file, Figures S9–S18). The much higher T_g of the slow-cooled rather than fast-cooled gel of 0.42 wt % **6** in silicone oil is consistent with its larger spherulites (Figure 6). However, the magnitude of the T_g difference for this gel, ca. 50 °C, is difficult to rationalize on the basis of the sizes of the **SAFIN** objects alone. XRD data presented later indicate that the

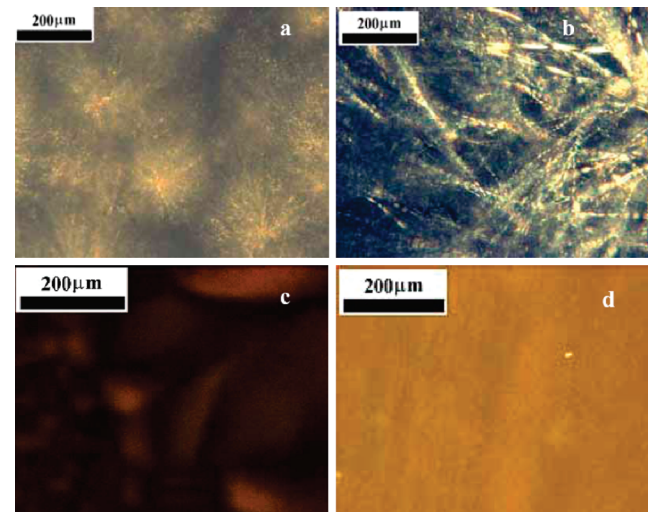


Figure 5. Polarizing optical micrographs at 24 °C of 2 wt % **1** in (a, b) silicone oil and (c, d) toluene gels prepared by (a, c) fast-cooling and (b, d) slow-cooling protocols. Both silicone oil micrographs show spherulitic textures.

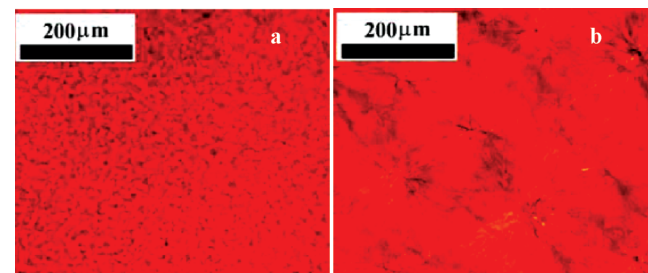


Figure 6. Polarizing optical micrographs at 24 °C of gels of 0.42 wt % **6** in silicone oil prepared by (a) fast-cooling and (b) slow-cooling protocols. The images were taken with a full-wave plate.

molecular packing within the objects of a fast-cooled gel with 5.0 wt % **6** in silicone oil differs from that of neat **6**. Unfortunately, the XRD method is not sufficiently sensitive to produce useful information on slow- and fast-cooled gels at 0.42 wt %. Also, for reasons that remain unclear, the gels of **1** in toluene prepared by the fast-cooling protocol exhibit a spherulitic texture (Figure 5c) whereas the **SAFIN** substructure in the slow-cooled gel is too small (<~2 μm) to be seen by our optical microscope (Figure 5d).

(27) Davey, R. J.; Garside, J. *From Molecules to Crystallizers*; Oxford University Press: New York, 2000; Chapter 2 and references cited therein.

(28) (a) Liu, X. Y.; Sawant, P. D. *Adv. Mater.* 2002, 14, 421–426. (b) Liu, X. Y.; Sawant, P. D. *Appl. Phys. Lett.* 2001, 79, 3518–3520.

(29) Rogers, M. A.; Marangoni, A. G. *Cryst. Growth Des.* 2008, 8, 4596–4601.

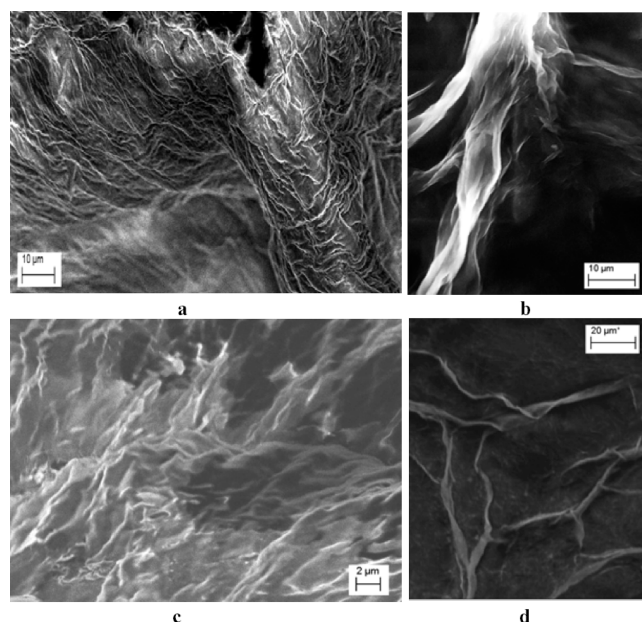


Figure 7. SEM images of xerogels prepared from (a) 2.0 wt % **1** in CCl_4 , (b) 0.5 wt % **1** in CCl_4 , (c) 2.0 wt % **1** in chlorobenzene, and (d) 0.5 wt % **1** in chlorobenzene. Scale bars are 10, 10, 2, and 20 μm in a–d, respectively.

We have also recorded the SEM images of xerogels prepared from representative gels (Figure 7). The micrographs from opaque gels of 2.0 and 0.5 wt % **1** in CCl_4 show fibrous structures, and that from 0.5 wt % **1** indicates that the fibers are helical (Figure 7b). Micrographs from transparent gels of 2.0 and 0.5 wt % **1** in chlorobenzene also show fibrous structures, including evidence of twisting in the more dilute sample (Figure 7c,d).

Molecular Packing within SAFIN Objects from X-ray Diffraction Data. XRD diffractograms of neat powders and fast-cooled silicone oil gels with 5 wt % **1**, **4**, **6**, **7**, **10**, **12**, and **13** have been compared. The diffraction peaks of the gels were identified by subtracting the amorphous scattering of the silicone oil from the total gel diffractogram.³⁰ The same morphology is present in the SAFINs of the gels and in the neat powders if the peaks in their diffractograms are found at the same values of 2θ , as is the case for **1** (Figure 8a,b). However, the correspondence is less clear for **4** and **6** (Figures 8c–f). The lattice spacings (d , Å) of the HSA derivatives in their crystalline and silicone oil gels have been calculated from the Bragg relationship and are summarized in Table 5. In all cases, attempts to index the diffraction peaks in Table 5 for **1**, **4**, **6**, **7**, **10**, **12**, and **13**³¹ and thereby to identify the gross natures of their cell packing were unsuccessful.

The Bragg distances of the low-angle peaks, indicative of lamellar packing, represent the thicknesses of the layers. For **1**, they are slightly less than twice the calculated extended molecular length³² (Table 5), suggesting a packing arrangement like that in Figure 9a. The positions of the diffraction peaks of the silicone oil gel of **4** correspond to that of the neat

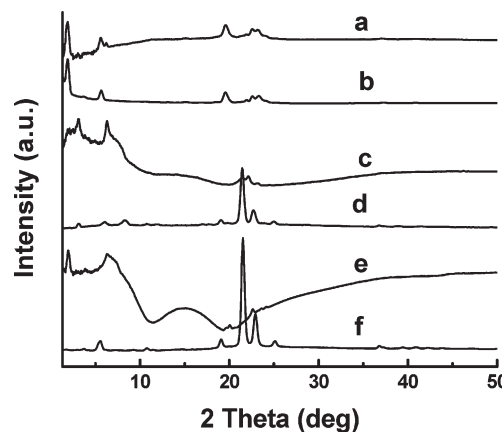


Figure 8. Vertically offset XRD patterns at 24 °C: (a) 4.8 wt % **1** in silicone oil gel after solvent subtraction; (b) neat **1**; (c) 5.2 wt % **4** in silicone oil gel after solvent subtraction; (d) neat **4**; (e) 5.0 wt % **6** in silicone oil gel after solvent subtraction; and (f) neat **6**.

powder, but the relative intensities within the two diffractograms differ as would be expected if the fibers of the SAFINs of **4** are oriented with respect to the capillary walls²⁴ (Figure 8c and Table 4). Consistent with a monolayer arrangement like that shown in Figure 9b, the distances corresponding to the lowest-angle peaks in the diffractograms are approximately the same as the calculated extended length of one molecule of **4**. Diffraction peaks of the silicone oil gel of the corresponding *N*-propyl amine, **10** (Supporting Information file, Figure S19), correlate with those of the neat powder as well.

Additional evidence for the same morphology of the LMOGs being present in the SAFINs and neat solid phases has been obtained from IR studies. The NH, OH, and CO stretching band frequencies of silicone oil gels with 5 wt % amide (**1** or **4**) are almost the same as those of the neat gelator (Supporting Information file, Figure S20). The NH stretching frequencies of the neat powder of amine **10** and its 5 wt % gel in silicone oil are also virtually the same. In addition, the sharpness of these IR peaks is consistent with specific H-bonding networks in the SAFIN fibers.

However, different diffraction peaks are found for the silicone oil gel and neat powder of both of the *N*-octadecyl LMOGs, **6** (Figure 8e,f) and **12** (Supporting Information file, Figure S21). For both gels, the lowest-angle peak in the XRD pattern corresponds approximately to the calculated extended length of one molecule and is consistent with a monolayer packing arrangement in the SAFINs (Figure 9c). The lowest-angle peaks observed correspond to distances that are less than one-half of the calculated molecular lengths. Thus, the data in hand are not consistent with a lamellar packing arrangement that is like any of the models in Figure 9. However, the diffractograms of the powders of **6** and **12** may be missing key peaks at angles lower than our diffractometer can record.

The diffraction pattern of the aggregates of **7** in its silicone oil gel (Supporting Information file, Figure S22) does not coincide with that of the neat powder. In the gel state, the low-angle peaks were very small even after exposure of the sample to X-rays for a period much longer than required to obtain good signal-to-noise ratios after solvent subtraction in the other gels at the same LMOG concentration. The layer spacing calculated from the analysis of the neat powder of **7** is slightly less than twice the

(30) Ostuni, E.; Kamaras, P.; Weiss, R. G. *Angew. Chem., Int. Ed.* **1996**, *35*, 1324–1326.

(31) Using JADE software from Materials Data Inc., Release 5.0.35 (SPS), Livermore, California.

(32) (a) Using Chem 3D Ultra 8 software (CambridgeSoft Corporation) and adding the van der Waals radii of the terminal atoms according to (b) Bondi, A. *J. Phys. Chem.* **1964**, *68*, 441–451.

Table 5. Comparison of Lattice Spacings (d , Å) of 1, 4, 6, 7, 10, 12, and 13 in their Neat Powders and Gels^a (from XRD Data at 24 °C) and Calculated Extended Molecular Lengths (L , Å)

	L^{32}	d (powder state)	d (gel state)
1	26.4	48.5, 15.7, 4.5, 3.9, 3.8	48.5, 15.7, 4.5, 3.9, 3.8
4	31.1	28.5, 14.3, 10.8, 8.2, 4.7, 4.1, 3.9, 3.6	28.5, 14.3, 4.2, 4.0, 3.8
6	50.3	23.8, 16.0, 12.2, 9.5, 8.8, 4.6, 4.1, 3.9, 3.5	46.5, 23.0, 14.0, 4.4, 3.9, 3.8, 3.7
7	27.2	47.1, 22.6, 17.2, 7.6, 7.3, 4.5, 4.2, 3.4, 3.1	17.4, 4.5, 4.1, 3.9
10	31.0	26.7, 13.6, 8.2, 6.5, 5.8, 5.0, 4.3, 4.1, 3.9, 3.6, 2.5, 2.4, 2.3	26.7, 13.6, 4.3, 4.1, 3.9, 3.6, 2.5, 2.3
12	50.2	16.0, 8.3, 7.5, 4.1, 3.7	47.7, 14.1, 4.1, 3.8
13	49.9	49.0, 16.9, 4.5, 4.1	49.0, 16.9, 4.5, 4.1

^a Gels prepared in silicone oil (~5 wt %) using the fast-cooling protocol.

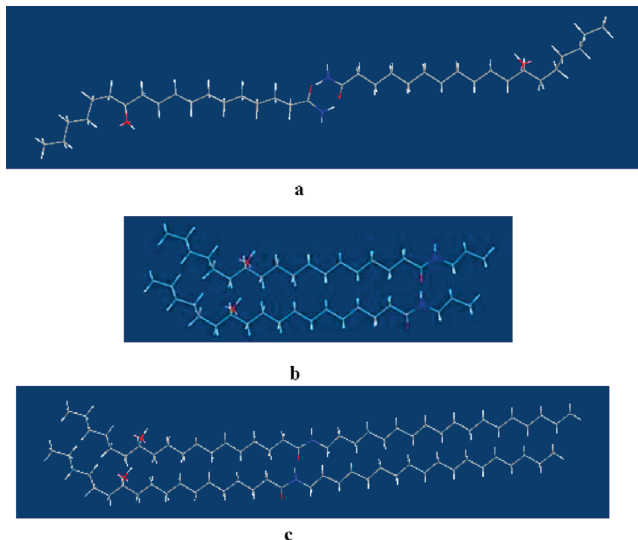


Figure 9. Proposed packing arrangements of gelator molecules in gel aggregates: (a) 1 (calculated molecular length of dimeric unit = 52.8 Å), (b) 4 (calculated molecular length = 31.1 Å), and (c) 6 (calculated molecular length = 50.3 Å) from molecular mechanics (MM2) calculations.³²

calculated extended molecular length, suggesting a bilayer packing arrangement. Finally, the X-ray diffractograms of the neat solid and silicone oil gel of the ammonium carbamate (**13**) indicate the same packing arrangement, probably stacked layers in which one ammonium and one carbamate are end-on (Table 4 and Supporting Information file, Figure S23).

Rheological Properties. The upper limit of the linear viscoelastic regime of a gel consisting of 2 wt % **1** in silicone oil was strain amplitude $\gamma \approx 0.1\%$ at angular frequency $\omega = 1 \text{ rad s}^{-1}$ at both 25 and 80 °C (Supporting Information file, Figure S24). Within this regime, the storage modulus (G') is 1 order of magnitude larger than the loss modulus (G'')—the gel is very stiff—and the G' and G'' values are independent of the applied frequency over a range of at least $\omega = 0.01–1.0 \text{ rad s}^{-1}$ from 25 to 80 °C (Supporting Information file, Figure S25). G'' and G' indicate that the gel becomes weaker with increasing temperature, perhaps as a result of more **1** being dissolved (Figure 4).

Strain sweep tests from $\gamma = 0.01$ to 100% at $\omega = 1 \text{ rad s}^{-1}$ were also performed for a 2 wt % **4** in silicone oil gel at 25 °C. The G' and G'' values remained approximately independent of applied strain up to 0.1%. Surprisingly, as the applied strain was increased at 45 or 75 °C, both G' and G'' increased initially (Supporting Information file, Figures S26 and S27). We attribute these observations to slow phase separation because the sample was visually a mixture of solid and liquid

after the experiment. A similar frequency sweep experiment on a 2 wt % **4** in silicone oil gel showed that G' and G'' are independent of the applied frequency at 25 and 35 °C but phase separation occurs at higher temperatures (Supporting Information file, Figure S28).

The G' and G'' values of a 2 wt % **10** in silicone oil gel decreased initially upon increasing strain at 25 and 50 °C ($\omega = 1.0 \text{ rad s}^{-1}$; Supporting Information file, Figure S29); the **10**/silicone oil gels are mechanically less stable than the corresponding **1** and **4** gels. At $\gamma = 0.05\%$ strain, G' and G'' of the 2 wt % **10** in silicone oil gel were independent of the applied frequency at different temperatures (Supporting Information file, Figure S30), thus confirming the viscoelasticity of the gel.

Thixotropic Properties. Usually, organogels from LMOGs, especially those in which the SAFINs are crystalline (as is the case here), are mechanically weak and are easily destroyed when subjected to external mechanical strain. Moreover, they are only weakly thixotropic, and after the cessation of severe mechanical strain, they can be reconstructed only by heating the mixture to its sol/solution state and cooling to below T_g . Several recent reports have attempted to explain the thixotropic behavior of LMOG-based organogels with crystalline SAFINs.³³ In all of these cases,^{33a} the restoration of the gel viscoelasticity, indicating at least some reestablishment of the SAFIN after mechanical disruption, required minutes to hours. Surprisingly, the recovery times of the gels in this work are much faster than previously reported in similar materials.

We measured the linear viscoelastic moduli, G' and G'' , for a 2 wt % **1** in silicone oil gel at 25 °C by performing oscillatory rheological measurements in a parallel plate geometry. At a strain amplitude of $\gamma = 0.1\%$ and angular frequency of $\omega = 100 \text{ rad s}^{-1}$, the gel is in the linear regime. Under these conditions, we measured the gel response for 150 s and saw no evolution of the moduli. Then, γ was increased to 30% while keeping ω fixed, resulting in a loss of elasticity (Supporting Information file, Figure S24). These conditions were applied for 30 s. Supporting Information file, Figure S31 shows the evolution of G' and G'' after γ is returned to the original conditions while maintaining $\omega = 100 \text{ rad s}^{-1}$. The kinetics of recovery were too rapid to be measured by the rheometer; ca. 90% of the original G' value (28 000 → 25 000 Pa) and ca. 96% of the original G''

(33) (a) Lescanne, M.; Grondin, P.; D'Aleo, A.; Fages, F.; Pozzo, J.-L.; Monval, O. M.; Reinheimer, P.; Collin, A. *Langmuir* **2004**, *20*, 3032–3041. (b) Brinksma, J.; Feringa, B. L.; Kellogg, R. M.; Vreeker, R.; Esch, J. V. *Langmuir* **2000**, *16*, 9249–9255. (c) Huang, X.; Raghavan, S. R.; Terech, P.; Weiss, R. *J. Am. Chem. Soc.* **2006**, *128*, 15341–15352. (d) Shirakawa, M.; Fujita, N.; Shinkai, S. *J. Am. Chem. Soc.* **2005**, *127*, 4164–4165. (e) Percec, V.; Peterca, M.; Yurchenko, M. E.; Rudick, J. G.; Heiney, P. A. *Chem.—Eur. J.* **2008**, *14*, 909–918.

Table 6. Comparison of the Degree of Thixotropy of HSA and Several of Its Derivatives at 2 wt % in Silicone Oil Gels at 25 °C

	% G' recovery ^{a,b}
HSA	69.8 ± 3.2
1	90.0 ± 1.0
2	45.0 ± 9.0
4	42.5 ± 14.2
10	3.8 ± 0.3
12	9.2 ± 4.6

^a Calculated from the ratio of the G' values after and before applying destructive strain (30% strain amplitude and 1 rad s⁻¹ for **HSA**, **1**, **12** and 100% strain amplitude and 1 rad s⁻¹ for **4** and **10**) for 30 s at 25 °C.

^b Average of three separate experiments.

value (8500 → 8100 Pa) were recovered in less than 10 s. Experiments with similar strain profiles, $\gamma = (50, 70, 90, \text{ and } 120)\%$ and $\omega = 1 \text{ rad s}^{-1}$ held for 30 s, demonstrate very similar results—the recovery of ca. 88% of the initial G' value in less than 10 s. Although the actual times and events responsible for this recovery may be partially due to instrumental factors and tool slip (i.e., a loss of contact between the sample and the metal plates of the rheometer), the rapid recovery does not appear to be an artifact of the measurement. To demonstrate this, a bulk sample of this gel was severely disturbed mechanically by moving a glass rod through it rapidly for more than 1 min. On all observable time scales, the material remained a gel without any qualitatively discernible change in its appearance or viscoelasticity.

Similar rheological measurements on silicone oil gels containing 2.0 wt % **HSA**, **2**, **4**, **10**, and **12** resulted in equally fast but somewhat lower recoveries of the original G' values (Table 6 and Supporting Information file, Figures S32–S36). The degrees of recovery correlate at least qualitatively with the potential strength of hydrogen-bonding interactions among the **LMOGs**: 1° amide (**1**) > acid (**HSA**) > 2° amides (**2**, **4**) > 2° amines (**10**, **12**).

As mentioned, a possible mechanism for the remarkably fast recovery times and, in several cases, high degrees of recovery of the viscoelastic properties includes slip or broken contacts between the **SAFINs** of the gels and the metal plates of the rheometer. To test this, we measured the recovery of G' for a gel that is only moderately thixotropic, 2 wt % **2** in silicone oil, at different plate separations. At all separations investigated (Table 7), the recovery was within the instrumental response time of the rheometer, < 10 s. We hypothesize that if slip or surface destruction of the gel were responsible for the rapid recovery, G' should decrease as the gap is increased. However, contrary to our expectations, G' increased as the plate gap decreased. Finally, an experiment with the same gel of **2** in silicone oil was performed using cone–plate geometry in which the strain is constant along the radius of the tool; there is a strain gradient along a radius in the plate–plate geometry. The results from the cone–plate geometry experiment are consistent with those from the 0.1 mm plate–plate gap experiment—ca. 85% recovery of G' in less than 10 s (Table 7).

Although the results in Table 6 point to the importance of hydrogen-bonding interactions, the mechanism of the recovery of these **SAFINs** remains unknown. In the sole literature precedent for such behavior in organogels with crystalline **SAFINs** that we have been able to find,^{33a} *N*-(3-hydroxypropyl) dodecanamide in toluene was transformed by applied strain from a jammed phase (a gel) to an aligned phase (a sol in which the fibers are no longer in an

Table 7. Comparison of the Thixotropic Properties of 2 wt % 2 in Silicone Oil Gel at 25 °C at Different Parallel Plate Separations and in Cone–Plate Geometry

geometry	gap (mm)	% G' recovery ^{a,b}
parallel plate	1.0	19.6 ± 1.6
parallel plate	0.5	45.0 ± 9.0
parallel plate	0.25	68.3 ± 0.9
parallel plate	0.1	83.0 ± 2.1
cone–plate	0.05 ^c	86.7 ± 2.3

^a Calculated from the ratio of the G' values after and before applying destructive strain (30% strain amplitude and 1 rad s⁻¹ for **2**) for 30 s at 25 °C. ^b Average from two separate experiments. ^c Closest contact of cone to plate.

effective 3D network). The rate of recovery of viscoelasticity after cessation of the destructive strain was dependent on the prior history of the sample, but the fastest recovery required a few minutes. The explanation given for these results may be applicable, at least in part, to our systems as well: the fibers of the **SAFIN** in the gel are joined by H-bonding interactions along their surfaces; the applied strain can break these interactions without destroying the fibers or a large part of their meso structures (N. B., spherulites in our **SAFINs**); and cessation of the destructive strain allows the aligned fibers (and spherulites) to diffuse rotationally and translationally to reform the **SAFIN** via renewed contacts. The fibrillar structures detected by optical and electron microscopy for the **LMOGs** in our study are compatible with such a mechanism, but they do not demand it.

General Discussion and Conclusions

The introduction of a hydroxyl group along the alkyl chain of stearic acid (a **b**-type molecule in Scheme 1), as in **HSA** (a **c**-type molecule), changes the gelating ability of an **LMOG** enormously. The efficiency of the **HSA**-derived gelators has been tuned further by modifying the carboxylic acid functionality of the head group, making it 1 of 13 different nitrogen-containing moieties. The efficiencies are improved when the carboxylic acid functionality is transformed into a primary amide (**1**, a **c**-type molecule), but efficiency suffers when a primary amine is placed in its stead (**7**, a different **c**-type molecule). Further changes of **1** to a secondary amide (**2** or **3**; molecules intermediate between **c**- and **d**-types) lead to decreased overall efficiencies, and increasing the alkyl chain length of the *N*-alkyl group of the secondary amide (i.e., from methyl in **2** to *N*-octadecyl in **6**, a **d**-type molecule) decreased the range of the liquids gelated further. Removal of the hydroxyl group in **1** yields stearamide (**14**, a **b**-type molecule), a very good **LMOG** that gelates a somewhat different set of liquids than **1** or **HSA**. The major differences in the gelated liquids can be understood on the basis of solubility considerations.

The importance of the ability of the head groups to act as both H-bonding donors and acceptors is demonstrated by the higher efficiency of the amides (**1–6**) than that of their corresponding amines (**7–12**) and ammonium carbamate **13**. Furthermore, the link between the ability to establish a strong H-bonding network along the octadecyl chains^{12a} and a robust **SAFIN** is indicated by comparisons of the gelator efficiencies of the **HSA** and corresponding **SA** derivatives. The IR spectral data are consistent with this interpretation because the NH, OH, and CO stretching bands are sharp (Supporting Information file, Figure S20), indicative of specific modes of H-bonding. However, our observation that the ammonium

carbamate with pendant hydroxy groups (**13**) is an inferior gelator to the one without hydroxy groups (**17**) suggests that the pendant group interactions are not always beneficial to gelation. Two possible reasons in the present case are (1) the secondary H-bonding network from the hydroxyl groups is established and imposes restraints on molecular packing that are not conducive to fiber (and **SAFIN**) formation and (2) the hydroxyl groups interact with the charged centers and lead to nonfibrous packing motifs.¹⁸

The primary headgroup interactions in the ammonium carbamate **13** are electrostatic in nature and, for that reason, potentially stronger than H-bonding in several of the low-polarity liquids gelated. However, **13** is a much less efficient gelator than the amides or amines. We suspect that the density of charges in the proximity of the head-group regions within the **SAFIN** fibers attenuates cationic–anionic charge stabilization. In other systems where the organization of charged head groups and their counterions within planes are known and the planes are separated by layers of long alkyl chains (as they appear to be here), the degree of stabilization is dependent on how well the opposite charges are able to adopt an alternating pattern.³⁴ Although we lack the structural information within the fibers of **13** to make a substantive model, we conjecture that such a pattern is not achieved in the fibers of **13**, perhaps as a consequence of packing constraints imposed by H-bonding networks of hydroxyl groups along the octadecyl chains.

As indicated by optical microscopy, differential scanning calorimetry, and X-ray diffractometry, the packing within the gel fibers of **1–13** is crystalline. Comparisons between X-ray diffractograms of the **SAFINs** of silicone oil gels and the neat powders of the **LMOGs** demonstrate that the same morphology is obtained in all cases except for **6** and **12**. Unfortunately, our efforts to grow diffraction-quality single crystals have not been successful thus far, and the exact nature of the packing within fibers is not known.²⁸ However, the low-angle diffraction peaks indicate that almost all of the **LMOGs** studied here pack in layers within their gel fibers.

Another interesting observation is that some of these organogels recover their viscoelasticity very rapidly after being destroyed by shear. For example, gels of 2 wt % **1** in silicone oil recovered ca. 90% of their original viscoelasticity within 10 s after the cessation of destructive shear, and several other gels recovered less viscoelasticity but equally fast. The fastest reversibility of which we are aware in other thixotropic organogels with crystalline **SAFINs** requires at least minutes.

Taken in total, our results suggest that the stabilization afforded by H-bonding in amide networks is the most important factor in determining stabilities within their

SAFINs. By limiting the H-bonding networks within a fiber to one donor per molecule, the *N*-alkyl groups of the secondary amides and amines also affect the shapes of the **SAFIN** fibers. In addition, the comparisons of gelator efficiency and stability when no, one, and two potentially strong anchoring points are placed along an alkane chain demonstrate that more is not always better! The stabilization gained when two or even several molecules aggregate can be lost when they are forced to pack efficiently in a crystalline matrix. The design of efficient gelators must take into consideration extended matrix effects, as has been done in a few examples thus far.^{1b,1d}

As a result of these attributes and the fact that organogels were formed at exceedingly low **LMOG** concentrations in a variety of liquids, these amides (and perhaps amines) may be useful as substitutes for **HSA** in its industrial applications,³⁵ or they may open the possibility of new applications. Perhaps most importantly is that the comparisons made among **HSA** and its derivatives **1–13** with **SA** and its derivatives **14–16**, both pairwise and in series, provide a comprehensive picture of the factors leading to the stability of these organogels. However, several unanticipated and challenging questions have arisen from the work presented here: there are general trends that can be extracted from correlations between the structure types in Scheme 1 and the properties of the gels formed, but a priori predictions of which **LMOG** will gel which liquid and what the properties of the gel will be remain elusive goals. That is the case even within the well-controlled series of simple **LMOG** structures examined here.

Acknowledgment. We thank the National Science Foundation for its support of this research.

Supporting Information Available: Material sources, syntheses, and characterizations of **1–13**. TGA plots of **7** and **13**. T_g values of toluene gels as a function of the concentration of **1** and **4**. Appearance and T_g values of gels of **14–17** in various liquids. Appearance and T_g values of several gels of **HSA** derivatives in silicone oil prepared by fast- and slow-cooling protocols. POM images of several gels prepared by fast- and slow-cooling protocols. XRD patterns of the silicone oil organogels of **7**, **10**, **12**, and **13** and their neat powders. IR spectra of the silicone oil gels of **1**, **4**, and **10**. log–log strain sweep plots of the silicone oil gels of **1**, **4**, and **10** and frequency sweeps of the silicone oil organogels of **4** and **10** at different temperatures. Time sweeps at 45 °C for a 2.0 wt % **4** in silicone oil gel. Thixotropic study of organogels of **HSA**, **1**, **2**, **4**, **10**, and **12** in silicone oil. This material is available free of charge via the Internet at <http://pubs.acs.org>.

(34) (a) Abdallah, D. J.; Bachman, R. E.; Perlstein, J.; Weiss, R. G. *J. Phys. Chem. B* **1999**, *103*, 9269–9278. (b) Abdallah, D. J.; Robertson, A.; Hsu, H. F.; Weiss, R. G. *J. Am. Chem. Soc.* **2000**, *122*, 3053–3062.

(35) Shankar, R.; Ghosh, T. K.; Spontak, R. J. *Soft Matter* **2007**, *3*, 1116–1129.